



## Assessment of rheological and microstructural changes of soluble fiber from chia seeds during an in vitro micro-digestion

Henry Lazaro<sup>a</sup>, Luis Puente<sup>a</sup>, Ma. Carolina Zúñiga<sup>b</sup>, Loreto A. Muñoz<sup>c,\*</sup>

<sup>a</sup> Universidad de Chile, Departamento de Ciencias de los Alimentos y Tecnología Química, Santos Dumont 964, Independencia, Santiago, Chile

<sup>b</sup> Universidad de Chile, Facultad de Cs. Químicas y Farmacéuticas, Depto. Química Orgánica y Analítica, Santos Dumont 964, Independencia, Santiago, Chile

<sup>c</sup> Universidad Central de Chile, Facultad de Ingeniería, 8330601, Santiago, Chile

### ARTICLE INFO

#### Keywords:

Chia seed  
*Salvia hispanica* L.  
 Mucilage  
 In vitro digestion

### ABSTRACT

The ability of some dietary fiber to increase the viscosity of digestive content may be associated with important positive implications in human health. An in vitro micro-digestion device was implemented to simulate and visualize the digestion of mucilage from chia seed. Changes in microstructure *in situ* and apparent viscosity were evaluated in 3, 5 and 8 g/kg concentrations of mucilage in three different digestions. The mucilage had a high-water holding capacity, approximately  $35.2 \pm 1.1$  g water/g mucilage. As the digestion processes progressed, the microstructure of the digesta changed from a compact sponge-like structure, with small pores forming an irregular network with average pore size of  $20.68 \pm 6.51$ ;  $40.90 \pm 7.45$  and  $15.50 \pm 6.07$   $\mu\text{m}$  to 3, 5 and 8 g/kg concentrations respectively, to a slightly less compact with average pore size that varies from  $19.87 \pm 7.00$   $\mu\text{m}$  in digestion 1 to  $29.79 \pm 15.47$   $\mu\text{m}$  in digestion 3.

A slight reduction in viscosity during the digestion process was observed; this behavior suggests that mucilage could maintain its structure in a food matrix and could be used to develop structured foods. Mucilage from chia seeds could be a potential functional ingredient with valuable attributes for food and nutraceutical industries.

### 1. Introduction

It is widely known that dietary fiber offers a multitude of beneficial properties to the health, its consumption has been associated with the prevention of cardiovascular diseases, obesity and cancer; plays an important role in gut health and can be used as “prebiotics”, between others benefits (Jenkins et al., 2002; Slavin, 2013; Slavin, Paredes-Diaz, & Fotopoulos, 2009). Dietary fiber has been defined such as primarily as the storage and cell wall polysaccharides of plants that cannot be hydrolyzed by human digestive enzymes (Marlett, McBurney, & Slavin, 2002) and depending on their behavior in aqueous solutions it is classified in soluble such as mucilages, pectins, gums, etc. and insoluble such as cellulose, lignin between others (Dhingra, Michael, Rajput, & Patil, 2012). In this context, the use of dietary fiber, soluble and/or insoluble, can be a useful tool in the development of structured foods matrices for health. Physical properties of the food matrix which include sensorial attributes, the structure breakdown upon digestion and stability, are largely dependent on the microstructure of the food matrix (Scholten, Moschakis, & Biliaderis, 2014); thus, the structure of foods should help manage and control the release of nutrients during the digestive process (Mela & Boland, 2014). Evidence indicates that

rheological properties of foods, such as physical and structural form, contribute to alter appetite and modulate glycemic responses (Zhu, Hsu, & Hollis, 2013), even, soluble gums are well known to induce viscosity and/or gelation and their physiological function has been often related with this property (Goff, Repin, Fabek, El Khoury, & Gidley, 2017). Conversely, other ingredients, such as fiber and other hydrocolloids (Kristensen & Jensen, 2011; Perrigue, Monsivais, & Drownowski, 2009), have shown that an increase in viscosity is associated with increased sensation of satiety (Flood, 2007, p. 182). Studies have also demonstrated that the effect of fiber-rich foods on physiological responses depends on hydration capacity, and these foods can increase the viscosity of human digesta (Vuksan et al., 2011). To modify the foods viscosity, industry has used different ingredients, such as proteins, polysaccharides, and gums, but until now, the mucilage from chia seed has been scarcely evaluated. *Salvia hispanica* L., more commonly known as chia seed, was an important food product in pre-Columbian societies (Muñoz, Cobos, Diaz, & Aguilera, 2012; Reyes Caudillo, Tecante, & Valdivia López, 2008). This oilseed is an important source of nutrients of great interest to food science and technology, due to its content of polyunsaturated fatty acids, proteins, dietary fiber and carbohydrates. Moreover, its mucilage, which is exuded when the seeds are soaked in

\* Corresponding author.

E-mail address: [loreto.munoz@uccentral.cl](mailto:loreto.munoz@uccentral.cl) (L.A. Muñoz).

water, corresponds to an anionic water-soluble heteropolysaccharide which has been tentatively identified as polymer of  $\beta$ -D-xylopyranosyl,  $\alpha$ -D-glucopyranosyl and 4-O-methyl- $\alpha$ -D-glucopyranosyluronic acid (Lin, Daniel, & Whistler, 1994). This polysaccharide is a good source of soluble fiber and has the ability to produce highly aqueous viscous dispersions, even at low concentrations (Muñoz et al., 2012; Timilsena, Adhikari, Kasapis, & Adhikari, 2015). One of the main physico-chemical properties of soluble fiber associated with the impact meaningfully digestion and absorption as well bolus transport are: viscosity, water holding capacity (WHC) and organic compound entrapment (Taghipoor, Barles, Georgelin, Licois, & Lescoat, 2014).

The aim of this work was to study the microstructural changes and apparent viscosity variations occurring during the digestion of three concentrations of crude mucilage from chia seed by using an in vitro micro-digestion device.

## 2. Materials and methods

### 2.1. Materials

Chia seeds without any previous treatment were provided by Benexia (Functional Products Trending S.A. Santiago, Chile). The enzymes and reagents for in vitro digestion: mucin from porcine stomach (EC 282-010-7, type II, code M2378), alpha-amylase from human saliva (EC 3.2.1.1, type IX-A, code A0521); pancreatin from porcine pancreas (EC 232-468-9, 8 x USP, code P7545); bile extract porcine (EC 232.369-0, code B8631), pepsin from porcine gastric mucosa (EC 3.4.23.1, lyophilized powder 3200–4500 units/mg protein code P6887) and trypsin from bovine pancreas (EC 3.4.21.4, type XI, lyophilized powder  $\geq$  6000 BAEE units/mg protein, code T1005) were purchased Sigma-Aldrich, St. Louis MO, USA.; sodium hydroxide (NaOH), EC 215-185-5, grade ACS.Reag. Ph Eur, Code 106469; hydrochloric acid (HCl) 5 mol/l, code 109911; sodium chloride (NaCl) (C 231-598-3, grade ACS, ISO, Reag., code 106404; potassium chloride (KCl) EC 231-211-8, for analysis, code 104936; calcium chloride (CaCl<sub>2</sub>) EC 233-140-8, Anhydrous powder Reag. Ph Eur, code 102378; sodium hydrogen carbonate (NaHCO<sub>3</sub>) EC 205-633-8, grade ACS,Reag. Ph Eur, code 106329 and ammonium carbonate (Na<sub>2</sub>CO<sub>3</sub>) EC 233-786-0, grade ACS,Reag. Ph Eur, code 159504 were purchased from Merck®.

### 2.2. Mucilage extraction and characterization

Mucilage was extracted from chia seeds by using the methodology proposed by Muñoz et al. (2012). Chia seeds were dispersed in deionized water in 1:40 seed:water ratio at room temperature (20 °C) under constant stirring during 2 h. Subsequently, the dispersion was dried at 50 °C for 10 h in an air convection heat oven. The dry crude mucilage was separated mechanically from the seed by rubbing over a 40-mesh sieve and stored in a sealed container at room temperature (20 °C) for subsequent analysis. Proximate analysis of crude mucilage was determined by using AOAC methods ((AOAC), 1995). Total carbohydrate content was determined by phenol-sulfuric acid method (BeMiller, 2010) and water holding capacity (WHC) was determined according to Sciarini et al. (2009) and expressed as g of water per g of dry crude mucilage (Sciarini, Maldonado, Ribotta, Pérez, & León, 2009).

$$WHC = \frac{W_s - W_d}{W_d}$$

Where  $W_s$  is the weight of swollen sample and  $W_d$  corresponds to dry sample. The analysis was performed in triplicate.

### 2.3. In vitro micro-digestion device

An in vitro device system was implemented to allow simulation and visualization of the digestion process (oral, gastric and intestinal) in real time (Fig. 1). The system was composed of a stereomicroscope (A)

(Olympus Optical CO, LTD, BX50F-3, Japan) and a digital camera (B) (TouCam, Industrial Digital Camera, UCMO508000KPA) connected to a computer (C). A micro-digester was placed on the stage (D) under the microscope. This micro-digester possessed a double concentric chamber, with outside (E) water recirculating at 37 °C; digestion was carried out inside a chamber (F) with 5 mL capacity. The outsider chamber was connected to a thermoregulated bath (RW-2025G, JEIO-TECH, Korea) at 37 °C to simulate body temperature for the micro-digester (G), and this bath was connected to a peristaltic pump controlled at 60 rpm (H) (Gibson, Minipuls Evolution 95400, Villiers Lebel, France). The external chamber was also connected to a syringe pump (NE-1000, New Era Pump Systems Inc., USA) with air injection and was controlled at 160 rpm depending on the digestion step (I) to simulate the peristaltic movements in the gastric and intestinal stages, respectively (Ekmekcioglu, 2002; Kellow, Borody, Phillips, Tucker, & Haddad, 1986). Digestion was conducted under a microscope (Fig. 1), and the data were registered and subsequently analyzed (J) by image analysis using ImageJ software (Schneider, Rasband, & Eliceiri, 2012).

### 2.4. Characterization of static in vitro digestion stages

Suspensions of 3, 5 and 8 g/kg mucilage from chia seed in triplicate were prepared in deionized water at 20 °C under constant stirring for 2 h. Three different digestions were performed in triplicate according with Table 1 to analyze how the mucilage is affected at different times of residence in each digestion step (digestion 1 shortest time and digestion 3 longest time). The times for the three digestions were determined according to reported by Hur et al. (2011), considering the maximum and minimum residence times reported in the literature for each digestion stage. The simulated saliva was prepared according to Kong & Singh (2008) by using gastric mucin (1 g/L),  $\alpha$ -amylase (2 g/L), NaCl (0.117 g/L), KCl (0.149 g/L) and NaHCO<sub>3</sub> (2.1 g/L) adjusted to pH 7 with NaOH (Kong & Singh, 2008).; Simulated gastric and intestinal juices were prepared according to Sanz and Luyten (2006) (Sanz & Luyten, 2006). The gastric juice was prepared by using pepsin (0.07 g/L) and trypsin (0.05 g/L), both derived from an electrolyte solution. The electrolyte solution was prepared with 53 mmol/L NaCl, 1 mmol/L CaCl<sub>2</sub>, 14.8 mmol/L KCl and 5.7 mmol/L Na<sub>2</sub>CO<sub>3</sub> at pH 2.5, adjusted with 2 mol/L HCl.

Simulated intestinal juice was prepared with an extract of pancreatine and bile. The extract of pancreatine and bile was prepared with 25 g of an electrolyte solution (21 mmol/L NaCl, 2 mmol/L KCl, and 0.5 mmol/L CaCl<sub>2</sub>); this solution was mixed with 7 g of pancreatin and 73 g of MilliQ water. This product was then mixed for 10 min and then centrifuged at 9800  $\times$  g at 4 °C for 20 min; finally, the supernatant was separated. The extract of pancreatine was prepared by mixing 0.475 g of bile in 25 mL of supernatant.

### 2.5. In vitro micro-digestion

The micro-digester was kept at 37 °C; then, 1000  $\mu$ L of each sample (3, 5 and 8 g/kg), also maintained at 37 °C, were injected respectively into the internal chamber. Subsequently, 250  $\mu$ L of recently prepared artificial saliva were added and the samples were maintained in the system for the time corresponding to the oral stage showed in Table 1 for each digestion. Once the oral stage was finished, 1000  $\mu$ L of gastric juice, adjusted to pH 2.5, were added to the mixture and maintained in the system for the time corresponding to the gastric stage (Table 1). The gastric stage was repeated for digestions 2 and 3 for each sample. In the gastric stage, the syringe pump was operated at 160 rpm to simulate peristaltic movements. After gastric digestion was completed, a 1250  $\mu$ L extract of pancreatin and bile were added, and then 50  $\mu$ L of trypsin were added, increasing the pH to 6.5 with 1 N NaHCO<sub>3</sub>. The mixture was mixed with a syringe pump using air injection at 4 mL/min for one minute, and subsequently, the pump was operated at 160 rpm to simulate peristaltic movements. The mixture was stirred for the time

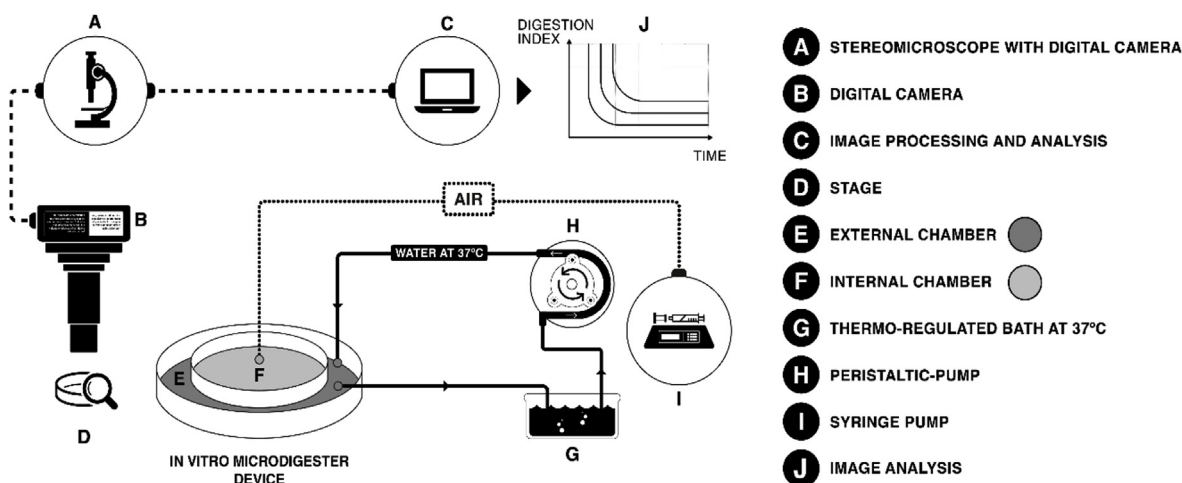


Fig. 1. Schem of micro-digestion dispositive.

Table 1

Digestion times.

Relative residence times at each digestion			
Digestion	Oral stage(s)	Gastric stage(min)	Intestinal stage (min)
1	20	20	40
2	30	30	80
3	40	40	120

corresponding to the intestinal stage showed in Table 1 at 37 °C. Fig. 2 shows a schematic representation of the static in vitro gastrointestinal digestion. Each concentration and digestion was performed in triplicate.

2.6. Image acquisition and microscopy analysis

Microstructural changes were registered by imaging acquisition at the beginning and the end of each digestion by a system composed of a stereomicroscope (Olympus Optical CO, LTD, BX50F-3, Japan) and a digital camera (ToupCam, Industrial Digital Camera, UCMO508000KPA). The camera was connected to a computer, which stored the images for subsequent analysis. The images were analyzed using ImageJ software. The microns scale was set in the software, after that the image was later binarized and the Feret's average diameter of the pores was determined in microns. (Schneider et al., 2012).

2.7. Steady shear flow behavior

The apparent viscosity to each concentration was determined in triplicate using a Hybrid Rheometer (Discovery HR-2, TA Instruments, USA) equipped with a 40 mm 2° cone-plate geometry and using a truncation gap of 50 μm and using the software TA Instruments Trios Version: 3.1.0.3538. The apparent viscosity was measured at 37 °C (simulating human body temperature) before and after each digestion at a shear rate ranging from 0.01 to 300 s<sup>-1</sup>. A sample without digestion for each concentration was used as a control. To simulate the dilution resulting from the digestion (250 μL of artificial saliva, 1000 μL of gastric juice and 1300 μL of intestinal juice) and to compare the viscosity between the samples, each control (3, 5 and 8 g/kg) was prepared in the same manner as the samples; to determine the viscosity, water was added in the same amount as the digestive fluids.

2.8. Statistical analysis

The results were expressed as the mean ± standard deviation calculated on three sample replicas. Comparisons among means were performed using Statgraphics XVI.I. The significant differences among the samples were performed using ANOVA and differences were considered significant at p < 0.05.

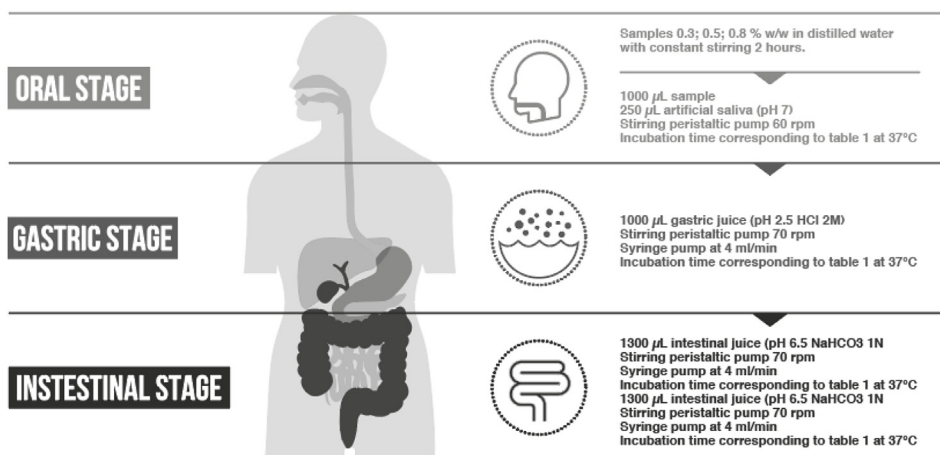


Fig. 2. Scheme of digestive process.

### 3. Results

#### 3.1. Mucilage extraction and characterization

The extracted crude mucilage represents an 8.3% of the seed. The proximate composition was  $8.2 \pm 0.3\%$  moisture,  $7.3 \pm 0.2\%$  ash;  $4.2 \pm 0.2\%$  protein and  $1.78 \pm 0.5\%$  lipids. The total carbohydrates was  $74.84 \pm 2.4\%$ , less than previously reported by [Timilsena, Adhikari, Kasapis, and Adhikari \(2016\)](#) presumably because it was a purified mucilage. Finally, the water holding capacity was  $35.2 \pm 1.1$  g/g. It is important to mention that the nutritional composition of chia seed and also mucilage content depends on many factors, such as genetics, climatic conditions and geographical locations where they were grown ([Ayerza & Coates, 2011](#)).

#### 3.2. In vitro digestion

The samples concentrations were selected under the basis to achieving low, medium and high apparent viscosities and considering that the crude mucilage at 1 g/kg is very difficult to handle due to its high consistency. The implementation of the dispositive allowed simulation and visualization of the gastro-intestinal digestion processes at real time. Until now, static in vitro systems have not allowed simulation of digestion with the possibility to observe and take images in real time. To acquire an image by using the traditional static in vitro digestion, the sample would need to be removed, potentially decreasing the temperature and affecting the structure of the material.

#### 3.3. Microscopy analysis

During the digestion progression, the structural changes in the mucilage produced by modifications in pH, ionic strength, enzymes and time were recorded by image acquisition during the different digestion stages in real time. [Fig. 3](#) shows the images taken before and after each digestion (1, 2 and 3 with different residence time) at the three concentrations; each image has a scale bar of 100  $\mu\text{m}$ . The three samples without digestion present an irregular sponge shape ([Fig. 3a, e and i](#)), with small pores forming an irregular network and fibril structures. In the sample at 3 g/kg concentration ([Fig. 3a](#)), the network appears more compact and flat (2D), the pores are more homogeneous with the average pore size was  $20.68 \pm 6.51$   $\mu\text{m}$ , likely due to the dilution. Samples without digestion at 5 and 8 g/kg ([Fig. 3 e and i](#)) exhibit a 3D shape with a sponge-like structure with pores of  $40.90 \pm 7.45$  and  $15.50 \pm 6.07$   $\mu\text{m}$ , respectively. This shape has been previously described as a fibrous structure by [Goh et al. \(2016\)](#) ([Goh et al., 2016](#)), as elongated microfibrils set in a network by [Salgado-Cruz et al. \(2013\)](#) ([Salgado-Cruz et al., 2013](#)) and as transparent mucilaginous dispersion composed by filamentous fiber forming branched structures by [Muñoz et al. \(2012\)](#).

As the digestion process progressed in the three digestions, the pores became larger, and the “sponge” structure appeared more open and less compact. This is more easily observed in the 3 g/kg sample ([Fig. 3b, c and d](#)) in the three digestions due to its greater dilution; it is presumed that this dynamic was produced by the action of the gastric and intestinal juices, which can access the structure more easily. The observed average pore size varied from  $19.87 \pm 7.00$   $\mu\text{m}$  in digestion 1 ([Figure 3b](#)) to  $29.79 \pm 15.47$   $\mu\text{m}$  in digestion 3 ([Fig. 3d](#)). However, in digestion 1, with shorter residence times ([Fig. 3b, f and j](#)) in all samples, the changes observed in the microstructure compared with the samples were not significantly different between the images before digestion; that is, the sponge-like structure remained almost intact. There was a notable change in the structure of digestions 2 and 3 for the 3 and 5 g/kg concentrations ([Fig. 3c, d, g and h](#)); this behavior is probably produced by longer times of residence for every digestion.

[Gidley \(2013\)](#) notes that hydrocolloids from plant cell walls resist enzymatic degradation in the stomach and small intestine and retain

their polymeric form. Nevertheless, this structure is affected when the times are longer, with the exception of the 8 g/kg dispersion in which the structure remains even with a long time of exposure for the gastric and intestinal juices ([Fig. 3k and l](#)). It is presumed that this behavior is because the higher concentration of mucilage produces an even denser and more compact structure that does not allow the access of enzymes and digestive juices. It is important to mention that the images were taken with an optical microscope, making it difficult to see 3D conformation; however, when the concentration was increased at 5 and 8 g/kg, the flatness of the surface decreased and the surface became rough. Moreover, at the 3 g/kg concentration, aggregates were observed; aggregates were also produced at the other concentrations but were not possible to see due to the compactness. The formation of these aggregates can be attributed to electrostatic interactions between the mucilage and traces of soluble proteins that could have solubilized during the mucilage extraction. This phenomenon was previously reported by [Scholten et al. \(2014\)](#), for example, oppositely charged protein-polysaccharide complexes ([Scholten et al., 2014](#)). Another explanation for the aggregate formation is the possible role of this anionic polysaccharide in intragastric structuring, similar to observations by [Soukoulis, Fisk, Gan, and Hoffmann \(2016\)](#) on anionic polysaccharides such as sodium alginate,  $\kappa$ -carrageenan and low methoxylpectin, where the mechanisms for intragastric structuring were ionotropic gelation, acid-self-structuring and thickening ([Soukoulis et al., 2016](#)).

#### 3.4. Steady shear flow behavior

As previously mentioned, the crude mucilage has a water holding capacity of  $35.2 \pm 1.1$  g/g, in agreement with [Timilsena et al. \(2015\)](#). When the mucilage comes into contact with water, it hydrates, swells and presents a form of fibrous microgel; similar behavior has been previously observed by several authors ([Goh et al., 2016](#); [Segura-Campos, Ciau-Solis, Rosado-Rubio, Chel-Guerrero, & Betancur-Ancona, 2014](#); [Timilsena et al., 2015](#)). Some physical properties of dietary fiber, such as water absorption capacity and dispersability, viscosity and ability to absorb/bind compounds, have shown to be related to physiological implications with important nutrition and health benefits ([Mackie, Rigby, Harvey, & Bajka, 2016](#); [Rana, Kumar Bachheti, Chand, & Barman, 2011](#)). The flow curves of the three concentrations of the mucilage from chia seeds at 37 °C before and after digestion are shown in [Fig. 4](#). As expected, the samples without digestion ([Fig. 4a](#)) showed a strong relation with concentration. The apparent viscosity shows a directly proportional relation to the concentration and decreases as the shear rate increases, resulting in a shear-thinning behavior. This behavior has been explained since as shear rate increases, the disarranged and partially aligned chains of the hydrocolloid become oriented and aligned resulting in a decrease of apparent viscosity ([Koocheki, Taherian, & Bostan, 2013](#)) Hence, the dispersions show pseudoplastic, non-Newtonian behavior, even at low concentrations, similar to the results of previous reports by [Capitani et al. \(2015\)](#) and [Timilsena et al. \(2015\)](#). In agreement with [Capitani et al. \(2015\)](#), the power law model was selected due to the model fitting the data, with an  $R^2$  value of 0.99. The differences observed between this study and the results of [Capitani et al. \(2015\)](#) and [Timilsena et al. \(2015\)](#) could be attributed to the difference in temperatures at which both were analyzed; in this study all samples were analyzed at 37 °C. In comparison with other soluble dietary fiber from mustard, flaxseed, oat and fenugreek those show Newtonian behavior at low concentrations, the crude mucilage exhibit pseudoplastic behavior even at low concentrations ([Repin, Cui, & Goff, 2018](#)). [Table 2](#) shows the parameters of the Power Law model, where  $K$  is the consistence index and  $n$  is the flow behavior index. The flow behavior index shows a value of  $n < 1$ , which agrees with pseudoplastic behavior and illustrates the dependence of samples' viscosity on shear rate. The flow behavior index  $n$  is similar to obtained by [Repin et al. \(2018\)](#) using fenugreek gum at similar concentrations, and comparable with dietary fiber from flaxseed and oat, those that were



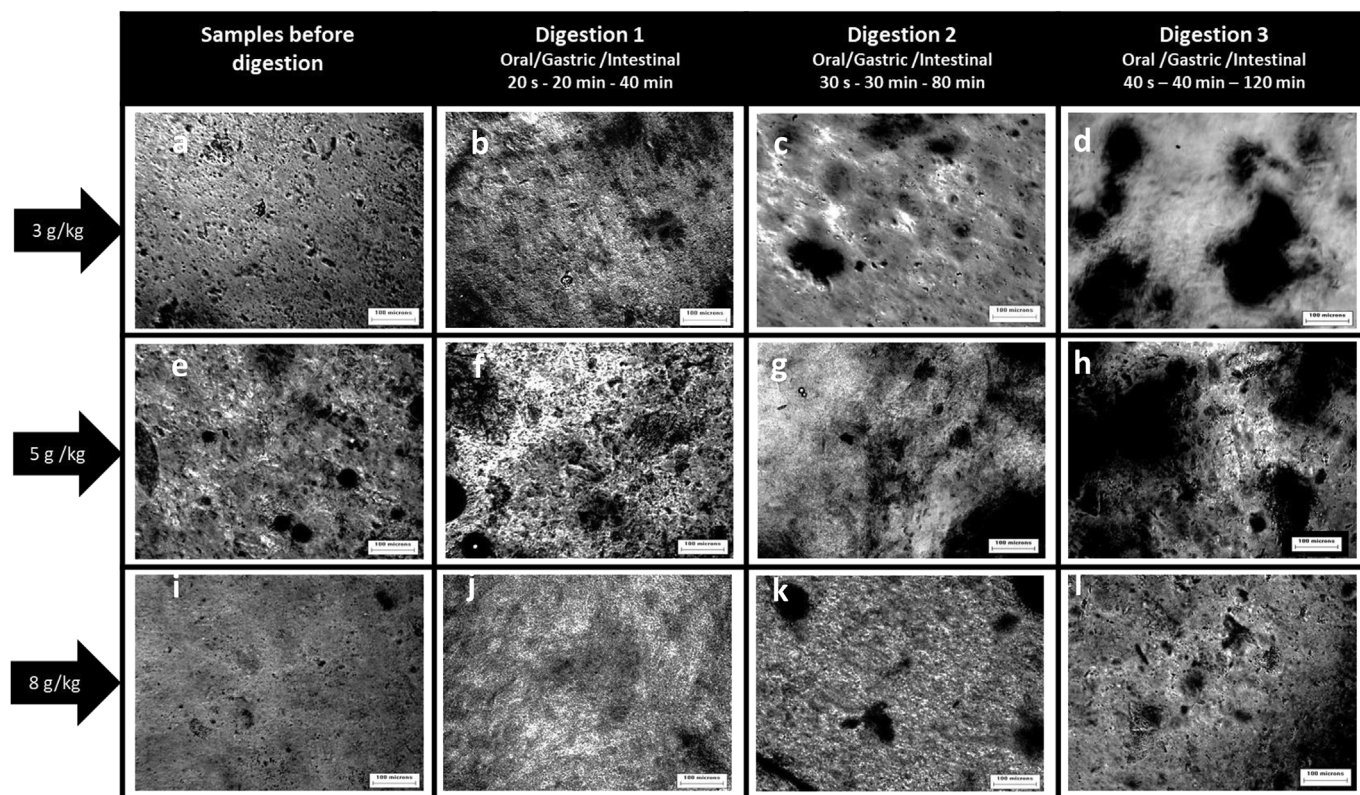


Fig. 3. Microstructure of the mucilage at different digestion conditions.

Fig. 3a refers to samples of 3 g/kg without digestion, while Figures b, c and d refers to samples of 3 g/kg at digestion 1, 2 and 3 respectively.

Fig. 3e refers to samples of 5 g/kg without digestion, while Figures f, g and h refers to samples of 5 g/kg at digestion 1, 2 and 3 respectively.

Fig. 3i refers to samples of 8 g/kg without digestion, while Figures j, k and l refers to samples of 8 g/kg at digestion 1, 2 and 3 respectively.

studied at higher concentrations. Furthermore, as predicted, an increase in the concentration results in an increase in the  $K$  value. Apparent viscosity between the 3 and 5 g/kg samples without digestion exhibits a similar behavior; however, the 8 g/kg sample shows higher viscosity. Apparent viscosities after digestion for each concentration are plotted in Fig. 4b, c and d. The apparent viscosity for the three mucilage concentrations under the lower digestion residence time exhibited a gradual and slightly decrease.

One of the most important parameters in viscosity reduction comparing samples with and without digestion was water dilution to simulate the volume of fluids during the digestion, similar to findings by Fabek et al. (2014) for several hydrocolloids. Other factors that may have influence in the change in viscosity can be attributed to the presence of small amount of soluble proteins released during the mucilage extraction and also, the digestion times, a longer residence time is associated with a greater reduction in viscosity. For the mucilage concentrations of 3 and 5 g/kg for digestion 1 (shorter residence time) observed in Fig. 4b and c, the changes in pH between the oral, gastric and intestinal steps and changes in hydrolytic enzymes did not result in significant changes in viscosity compared with the corresponding sample-dilution at each concentration. However, in Fig. 4 b and c (3 and 5 g/kg concentration) the curves to digestion 1 at shear rate lower than 50 s<sup>-1</sup> are slightly higher than the samples without digestion; this increase in digesta viscosity has been explained previously by Gidley et al. (2013) and Fabek et al. (2014) such as a direct result of the inherent ability of the polymer chains to overlap with each other creating a greater number of junction zones due to the influence of fluctuations of pH, presence of electrolytes, enzymes and bile salt concentrations. Various authors have reported the association between increases in the viscosity of digesta produced by some polysaccharides and delayed gastric emptying and other beneficial physiological effects, including

satiating (Blackwood, Salter, Dettmar, & Chaplin, 2000; Kristensen & Jensen, 2011; Vuksan et al., 2011).

In a study conducted by Clark and Slavin (2013) where different kinds of fiber were studied, it was determined that intragastric viscosity could play an important role in satiety. Additionally, Norton et al. (2015) noted that the viscosity of the food matrix can affect digestive motility, delaying gastric emptying and intestinal transit and thus affecting the rate at which nutrients are released or absorbed. This finding agrees with prior research by Hardacre et al. (2015); the presence of significant quantities of soluble or insoluble fiber in the diet increases the viscosity of digesta and likely reduces the rate of liberated nutrients to sites of absorption. According to Goh et al. (2016), the viscosity produced by aqueous suspensions of mucilage from chia seeds can control the movements of digesta through the gastrointestinal tract.

Moreover, the slight reduction in the viscosity during the digestion process suggests that mucilage can resist acidic environments and enzymatic degradation; furthermore, the ability of mucilage to maintain its structure could be used to structure foods to slow digestion, in agreement with the work of Gidley (2013).

### 3.5. Conclusions

This polysaccharide offers promise as a functional ingredient to be used in structured foods, providing potential health benefits such as soluble fiber. Crude mucilage has a high capacity for water absorption and forms viscous dispersions even at low concentrations; this characteristic makes it attractive for the food and nutraceutical industry as an ingredient that could enable the design of structured food products for health and wellness.

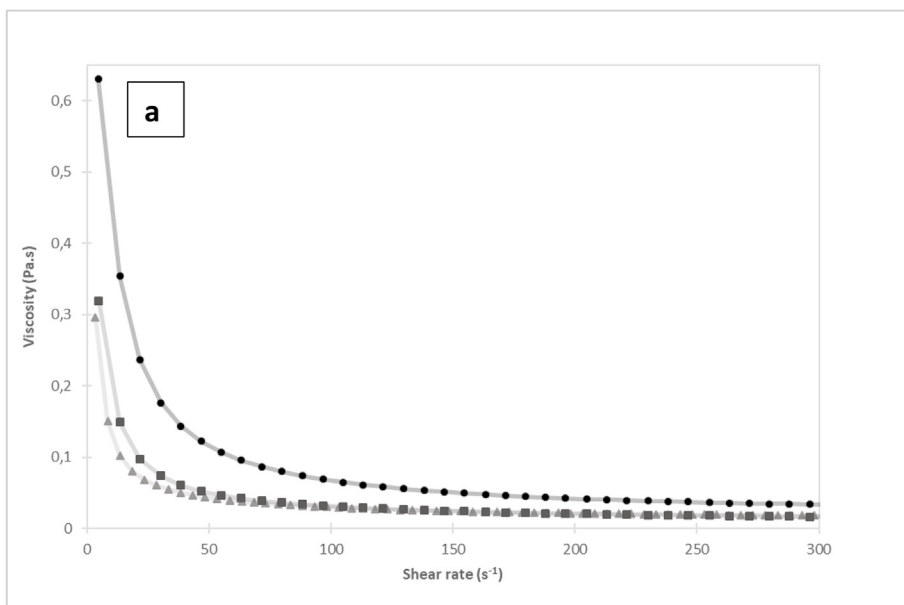


Fig. 4. Apparent viscosity of mucilage from chia seed at 37 °C before and after digestion.

Fig. 4a. Flow behavior of samples of mucilage from chia seeds without digestion. The symbol (Δ) 3 g/kg; the symbol (■) 5 g/kg and the symbol (●) 8 g/kg.

Fig. 4b. Flow behavior of samples of mucilage at 3. g/kg; (Δ) diluted samples; (■) digestion 1, (◆) digestion 2 and (●) digestion 3.

Fig. 4c. Flow behavior of samples of mucilage at 5. g/kg; (Δ) diluted samples; (■) digestion 1, (◆) digestion 2 and (●) digestion 3.

Fig. 4d. Flow behavior of samples of mucilage at 8 g/kg; (Δ) diluted samples; (■) digestion 1, (◆) digestion 2 and (●) digestion 3.

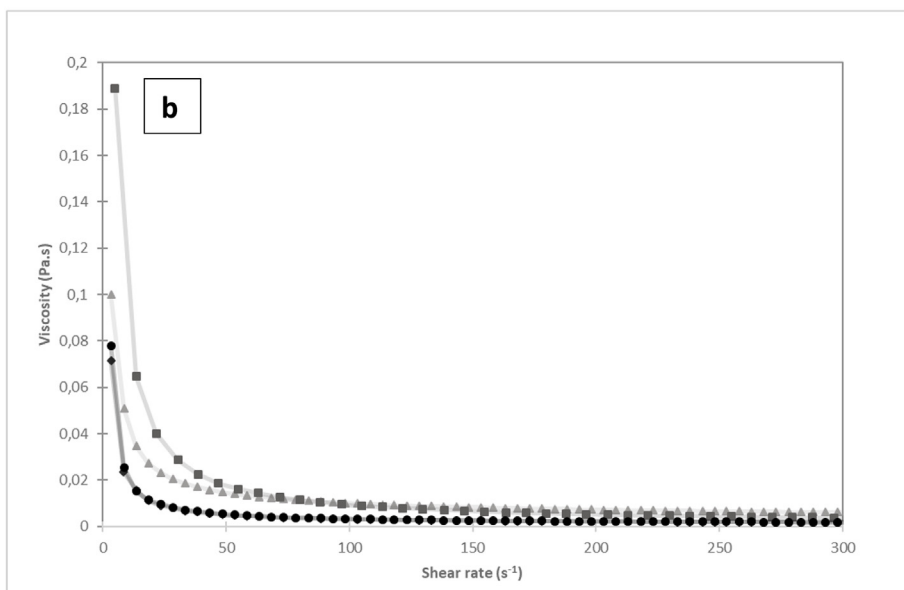


Table 2  
Power of Law parameters.

Sample concentration	K (Pa.s)	n	R <sup>2</sup>
0.3%	0.71 <sup>a</sup>	0.38 <sup>a</sup>	0.99
0.5%	0.76 <sup>a</sup>	0.42 <sup>a</sup>	0.99
0.8%	0.82 <sup>b</sup>	0.58 <sup>b</sup>	0.98

The values represent the mean ± standard deviation of triplicate tests, The values represent the mean ± standard deviation of triplicate tests. Different letters mean significant differences (p < 0.05).

**Acknowledgments**

The authors acknowledge the financial support of FONDECYT Project 11150307 from the Chilean National Commission for Science and Technological Research (CONICYT).

**References**

(AOAC), A. o. O. A. C (1995). *Official methods of analysis* (16th ed.). Washigton DC: AOAC International.

Ayerza, R., & Coates, W. (2011). Protein content, oil content and fatty acid profiles as potential criteria to determine the origin of commercially grown chia (*Salvia hispanica* L.). *Industrial Crops and Products*, 34(2), 1366–1371. <https://doi.org/10.1016/j.indcrop.2010.12.007>.

BeMiller, J. N. (2010). Carbohydrate analysis. In S. Nielsen (Ed.). *Food analysis* (pp. 147–175). (4th ed.). New York, USA: Springer.

Blackwood, A. D., Salter, J., Dettmar, P. W., & Chaplin, M. F. (2000). Dietary fibre, physicochemical properties and their relationship to health. *Journal of the Royal Society for the Promotion of Health*, 120(4), 242–247. <http://dx.doi.org/10.1177/146642400012000412>.

Capitani, M. I., Corzo-Rios, L. J., Chel-Guerrero, L. A., Betancur-Ancona, D. A., Nolasco, S. M., & Tomás, M. C. (2015). Rheological properties of aqueous dispersions of chia (*Salvia hispanica* L.) mucilage. *Journal of Food Engineering*, 149, 70–77. <http://dx.doi.org/10.1016/j.jfoodeng.2014.09.043>.

Clark, M. J., & Slavin, J. L. (2013). The effect of fiber on satiety and food intake: A systematic review. *Journal of the American College of Nutrition*, 32(3), 200–211. <http://dx.doi.org/10.1080/07315724.2013.791194>.

Dhingra, D., Michael, M., Rajput, H., & Patil, R. T. (2012). Dietary fibre in foods: A review. *Journal of Food Science & Technology*, 49(3), 255–266. <http://dx.doi.org/10.1007/s13197-011-0365-5>.

Ekmekcioglu, C. (2002). A physiological approach for preparing and conducting intestinal

- bioavailability studies using experimental systems. *Food Chemistry*, 76(2), 225–230. [http://dx.doi.org/10.1016/S0308-8146\(01\)00291-6](http://dx.doi.org/10.1016/S0308-8146(01)00291-6).
- Fabek, H., Messerschmidt, S., Brulport, V., & Goff, H. D. (2014). The effect of in vitro digestive processes on the viscosity of dietary fibres and their influence on glucose diffusion. *Food Hydrocolloids*, 35, 718–726. <http://dx.doi.org/10.1016/j.foodhyd.2013.08.007>.
- Flood, J. E. (2007). *The effects of the form of food on energy intake and satiety* Doctor of Philosophy PhD Thesis. Pennsylvania: The Pennsylvania State University.
- Gidley, M. J. (2013). Hydrocolloids in the digestive tract and related health implications. *Current Opinion in Colloid & Interface Science*, 18(4), 371–378. <http://dx.doi.org/10.1016/j.cocis.2013.04.003>.
- Goff, H. D., Repin, N., Fabek, H., El Khoury, D., & Gidley, M. J. (2017). Dietary fibre for glycaemia control: Towards a mechanistic understanding. *Bioactive Carbohydrates and Dietary Fibre*. <http://dx.doi.org/10.1016/j.bcdf.2017.07.005>.
- Goh, K. K. T., Matia-Merino, L., Chiang, J. H., Quek, R., Soh, S. J. B., & Lentle, R. G. (2016). The physico-chemical properties of chia seed polysaccharide and its microgel dispersion rheology. *Carbohydrate Polymers*, 149, 297–307. <http://dx.doi.org/10.1016/j.carbpol.2016.04.126>.
- Hardacre, A. K., Yap, S.-Y., Lentle, R. G., & Monro, J. A. (2015). The effect of fibre and gelatinised starch type on amylolysis and apparent viscosity during in vitro digestion at a physiological shear rate. *Carbohydrate Polymers*, 123, 80–88. <http://dx.doi.org/10.1016/j.carbpol.2015.01.013>.
- Hur, S. J., Lim, B. O., Decker, E. A., & McClements, D. J. (2011). In vitro human digestion models for food applications. *Food Chemistry*, 125(1), 1–12. <http://dx.doi.org/10.1016/j.foodchem.2010.08.036>.
- Jenkins, D. J., Kendall, C. W., Vuksan, V., Vidgen, E., Parker, T., Faulkner, D., et al. (2002). Soluble fiber intake at a dose approved by the US food and drug administration for a claim of health benefits: Serum lipid risk factors for cardiovascular disease assessed in a randomized controlled crossover trial. *American Journal of Clinical Nutrition*, 75(5), 834–839. <http://dx.doi.org/10.1093/ajcn/75.5.834>.
- Kellow, J. E., Borody, T. J., Phillips, S. F., Tucker, R. L., & Haddad, A. C. (1986). Human interdigestive motility: Variations in patterns from esophagus to colon. *Gastroenterology*, 91, 386–395. [http://dx.doi.org/10.1016/0016-5085\(86\)90573-1](http://dx.doi.org/10.1016/0016-5085(86)90573-1).
- Kong, F., & Singh, R. P. (2008). A model stomach system to investigate disintegration kinetics of solid foods during gastric digestion. *Journal of Food Science*, 73(5), E202–E210. <http://dx.doi.org/10.1111/j.1750-3841.2008.00745.x>.
- Koocheki, A., Taherian, A. R., & Bostan, A. (2013). Studies on the steady shear flow behavior and functional properties of Lepidium perfoliatum seed gum. *Food Research International*, 50(1), 446–456. <http://dx.doi.org/10.1016/j.foodres.2011.05.002>.
- Kristensen, M., & Jensen, M. G. (2011). Dietary fibres in the regulation of appetite and food intake. Importance of viscosity. *Appetite*, 56(1), 65–70. <http://dx.doi.org/10.1016/j.appet.2010.11.147>.
- Lin, K. Y., Daniel, J. R., & Whistler, R. L. (1994). Structure of chia seed polysaccharide exudate. *Carbohydrate Polymers*, 23(1), 13–18. [http://dx.doi.org/10.1016/0144-8617\(94\)90085-X](http://dx.doi.org/10.1016/0144-8617(94)90085-X).
- Mackie, A., Rigby, N., Harvey, P., & Bajka, B. (2016). Increasing dietary oat fibre decreases the permeability of intestinal mucus. *Journal of Functional Foods*, 26, 418–427. <http://dx.doi.org/10.1016/j.jff.2016.08.018>.
- Marlett, J. A., McBurney, M. I., & Slavin, J. L. (2002). Position of the american dietetic Association: Health implications of dietary fiber. *Journal of the American Dietetic Association*, 102(7), 993–1000. [http://dx.doi.org/10.1016/S0002-8223\(02\)90228-2](http://dx.doi.org/10.1016/S0002-8223(02)90228-2).
- Mela, D. J., & Boland, M. J. (2014). Applying structuring approaches for satiety: Challenges faced, lesson learned. In M. Boland, M. Golding, & H. Singh (Eds.). *Food structures, digestion and health* (pp. 363–388). San Diego, USA: Elsevier Inc.
- Muñoz, L. A., Cobos, A., Diaz, O., & Aguilera, J. M. (2012). Chia seeds: Microstructure, mucilage extraction and hydration. *Journal of Food Engineering*, 108(1), 216–224. <http://dx.doi.org/10.1016/j.jfoodeng.2011.06.037>.
- Norton, J. E., Gonzalez Espinosa, Y., Watson, R. L., Spyropoulos, F., & Norton, I. T. (2015). Functional food microstructures for macronutrient release and delivery. *Food & Function*, 6(3), 663–678. <http://dx.doi.org/10.1039/C4FO00965G>.
- Perrigue, M. M., Monsivais, P., & Drewnowski, A. (2009). Added soluble fiber enhances the satiating power of low-energy-density liquid yogurts. *Journal of the American Dietetic Association*, 109(11), 1862–1868. <http://dx.doi.org/10.1016/j.jada.2009.08.018>.
- Rana, V., Kumar Bachheti, R., Chand, T., & Barman, A. (2011). Dietary fibre and human health. *International Journal of Food Safety, Nutrition and Public Health*, 4(2/3/4), 101–108. <http://dx.doi.org/10.1504/IJFSNPH.2011.044528>.
- Repin, N., Cui, S. W., & Goff, H. D. (2018). Rheological behavior of dietary fibre in simulated small intestinal conditions. *Food Hydrocolloids*, 76(Supplement C), 216–225. <http://dx.doi.org/10.1016/j.foodhyd.2016.10.033>.
- Reyes Caudillo, E., Tecante, A., & Valdivia López, M. A. (2008). Dietary fibre content and antioxidant activity of phenolic compounds present in Mexican chia (*Salvia hispanica* L.) seeds. *Food Chemistry*, 107(2), 656–663. <http://dx.doi.org/10.1016/j.foodchem.2007.08.062>.
- Salgado-Cruz, M. d. l. P., Calderón-Domínguez, G., Chanona-Pérez, J., Farrera-Rebollo, R. R., Méndez-Méndez, J. V., & Díaz-Ramírez, M. (2013). Chia (*Salvia hispanica* L.) seed mucilage release characterisation. A microstructural and image analysis study. *Industrial Crops and Products*, 51, 453–462. <http://dx.doi.org/10.1016/j.indcrop.2013.09.036>.
- Sanz, T., & Luyten, H. (2006). Effect of thickening agent in the in vitro mouth, stomach and intestine release of tyrosol from enriched custards. *Food Hydrocolloids*, 20(5), 703–711. <http://dx.doi.org/10.1016/j.foodhyd.2005.06.013>.
- Schneider, C. A., Rasband, W. S., & Eliceiri, K. W. (2012). NIH image to ImageJ: 25 years of image analysis. *Nature Methods*, 9(7), 671–675. <http://dx.doi.org/10.1038/nmeth.2089>.
- Scholten, E., Moschakis, T., & Biliaderis, C. G. (2014). Biopolymer composites for engineering food structures to control product functionality. *Food Structure*, 1(1), 39–54. <http://dx.doi.org/10.1016/j.foostr.2013.11.001>.
- Sciarini, L. S., Maldonado, F., Ribotta, P. D., Pérez, G. T., & León, A. E. (2009). Chemical composition and functional properties of Gleditsia triacanthos gum. *Food Hydrocolloids*, 23(2), 306–313. <http://dx.doi.org/10.1016/j.foodhyd.2008.02.011>.
- Segura-Campos, M. R., Ciau-Solis, N., Rosado-Rubio, G., Chel-Guerrero, L., & Betancur-Ancona, D. (2014). Chemical and functional properties of chia seed (*salvia hispanica* L.) gum. *International Journal of Food Science*, 2014. <http://dx.doi.org/10.1155/2014/241053> 5 pages.
- Slavin, J. (2013). Fiber and Prebiotics: Mechanisms and health benefits. *Nutrients*, 5(4), 1417–1435. <http://dx.doi.org/10.3390/nu5041417>.
- Slavin, J. V. S., Paredes-Diaz, A., & Fotopoulos, G. (2009). A review of the role of soluble fiber in health with specific reference to wheat dextrin. *Journal of International Medical Research*, 37(1), 1–17. <http://dx.doi.org/10.1177/147323000903700101>.
- Soukoulis, C., Fisk, I. D., Gan, H.-H., & Hoffmann, L. (2016). Intra-gastric structuring of anionic polysaccharide kappa-carrageenan filled gels under physiological in vitro digestion conditions. *Journal of Food Engineering*, 191, 105–114. <http://dx.doi.org/10.1016/j.jfoodeng.2016.07.009>.
- Taghipoor, M., Barles, G., Georgelin, C., Licois, J. R., & Lescoat, P. (2014). Digestion modeling in the small intestine: Impact of dietary fiber. *Mathematical Biosciences*, 258(Supplement C), 101–112. <http://dx.doi.org/10.1016/j.mbs.2014.09.011>.
- Timilsena, Y. P., Adhikari, R., Kasapis, S., & Adhikari, B. (2015). Rheological and microstructural properties of the chia seed polysaccharide. *International Journal of Biological Macromolecules*, 81, 991–999. <http://dx.doi.org/10.1016/j.ijbiomac.2015.09.040>.
- Timilsena, Y. P., Adhikari, R., Kasapis, S., & Adhikari, B. (2016). Molecular and functional characteristics of purified gum from Australian chia seeds. *Carbohydrate Polymers*, 136, 128–136. <http://dx.doi.org/10.1016/j.carbpol.2015.09.035>.
- Vuksan, V., Jenkins, A. L., Rogovik, A. L., Fairgrieve, C. D., Jovanovski, E., & Leiter, L. A. (2011). Viscosity rather than quantity of dietary fibre predicts cholesterol-lowering effect in healthy individuals. *British Journal of Nutrition*, 106(9), 1349–1352. <http://dx.doi.org/10.1017/S0007114511001711>.
- Zhu, Y., Hsu, W. H., & Hollis, J. H. (2013). The impact of food viscosity on eating rate, subjective appetite, glycemic response and gastric emptying rate. *PLoS One*, 8(6), 1–6.